



A novel injection technique: using a field-based quantum cascade laser for the analysis of gas samples derived from static chambers

Anne R. Wecking¹, Vanessa M. Cave², Liyǐn L. Liáng³, Aaron M. Wall¹, Jiafa Luo², David I. Campbell¹,
 Louis A. Schipper¹

¹ School of Science and Environmental Research Institute, The University of Waikato, Private Bag 3105,
 Hamilton 3240, Aotearoa New Zealand

² AgResearch Ruakura, Private Bag 3123, Hamilton 3240, Aotearoa New Zealand

³ Manaaki Whenua – Landcare Research, Palmerston North 4442, Aotearoa New Zealand

Correspondence to: Anne R. Wecking (arw35@students.waikato.ac.nz), Louis A. Schipper (louis.schipper@waikato.ac.nz)

Abstract. The development of fast-response analysers for the measurement of nitrous oxide (N₂O) has resulted in exciting opportunities for new experimental techniques beyond commonly used static chambers and gas chromatography (GC) analysis. For example, quantum cascade laser absorption spectrometers (QCL) are now being used with eddy covariance (EC) or automated chambers. However, using a field-based QCL EC system to also quantify N₂O concentrations in gas samples taken from static chambers has not yet been explored. Gas samples from static chambers are commonly analysed by GC that often requires labour and time consuming procedures off-site. Here, we developed a novel, field-based injection technique that allowed the use of a single QCL for: 1) micrometeorological EC; and 2) immediate manual injection of headspace samples taken from static chambers. To test this approach across a range of low to high N₂O fluxes, we applied ammonium nitrate (AN) at 0, 300, 600 and 900 kg N ha⁻¹ (AN₀, AN₃₀₀, AN₆₀₀, AN₉₀₀) to plots on a pasture soil. After analysis, calculated N₂O fluxes from QCL (F_{N₂O_QCL}) were compared with fluxes determined by a standard method, i.e. here laboratory-based GC (F_{N₂O_GC}). Subsequent comparison of QCL and GC derived data was tested using orthogonal regression, Bland Altman and bioequivalence statistics. For the AN treated plots, the mean cumulative N₂O emissions across the seven day campaign were 0.97 (AN₃₀₀), 1.26 (AN₆₀₀) and 2.00 (AN₉₀₀) kg N₂O-N ha⁻¹ for F_{N₂O_QCL} and 0.99 (AN₃₀₀), 1.31 (AN₆₀₀) and 2.03 (AN₉₀₀) kg N₂O-N ha⁻¹ for F_{N₂O_GC}. These F_{N₂O_QCL} and F_{N₂O_GC} were highly correlated (r = 0.996, n = 81) based on orthogonal regression, in agreement following the Bland Altman approach (i.e. within ± 1.96 standard deviations of the mean difference) and shown to be for all intents and purposes the same (i.e. bioequivalent). The F_{N₂O_QCL} and F_{N₂O_GC} derived under near-zero flux conditions (AN₀) were weakly correlated (r = 0.306, n = 27) and not found to agree or to be bioequivalent. This was likely caused by the calculation of small but apparent positive and negative F_{N₂O} when in fact the actual flux was zero, i.e. below the detection limit of static chambers. Our study demonstrated (1) that the capability of using one QCL to measure N₂O at different scales, including manual injections, offered a great potential to advance field measurements of N₂O (and other greenhouse gases) in future; and (2) that suitable statistics have to be adopted when formally assessing the agreement and difference (not only the correlation) between two methods of measurement.



1 Introduction

Accurate measurements of nitrous oxide (N_2O) emissions from agricultural land are crucial to quantify the contribution of the gas's radiative forcing to climate warming (Thompson et al., 2019). Nitrous oxide is a long-lived greenhouse gas with a global warming potential 265-times higher than that of carbon dioxide (CO_2) over 100 years, and is the largest contributor to the depletion of stratospheric ozone (IPCC, 2013; Ravishankara et al., 2009). Agricultural activities on intensively managed soils that receive high inputs of reactive nitrogen (N_r), mostly in the form of animal excreta and nitrogen fertiliser, are the main source of anthropogenic N_2O emissions (Reay et al., 2012). Reactive nitrogen facilitates microbial nitrification and denitrification in the soil with N_2O being an intermediate of these processes (Butterbach-Bahl et al., 2013; Firestone and Davidson, 1989). The production of N_2O in soils is controlled by a multitude of environmental and anthropogenic factors, e.g. soil moisture, nitrogen input and overall farm management, which often result in highly variable N_2O emissions (Erismann et al., 2013; Flechard et al., 2007; Rees et al., 2013). Adequate and precise flux measurements have, therefore, remained challenging (Cowan et al., 2020; Rapson and Dacres, 2014).

To date, the common method for measuring fluxes of N_2O ($F_{\text{N}_2\text{O}}$) are closed, non-steady-state 'static chambers' (Hutchinson and Mosier, 1981; Lundegard, 1927); a method used for more than 95 % of all field measurements (Lammirato et al., 2018; Rochette and Eriksen-Hamel, 2008; Rochette, 2011). Static chambers are relatively cost-efficient and easy to deploy in the field (de Klein et al., 2015; Velthof et al., 1996). Gas samples are extracted from the chamber headspace during an up to 60 min enclosure and injected into pre-evacuated glass vials (Luo et al., 2007; Rochette and Bertrand, 2003; van der Weerden et al., 2011). Subsequent analysis of the gas samples is commonly conducted off-site, using gas chromatography (GC) (Luo et al., 2008a; Parkin and Venterea, 2010). However, measurements using static chambers are discontinuous and labour-intensive with uncertainties in $F_{\text{N}_2\text{O}}$ caused by alterations made to the soil environment after installation, pressure differences in the chamber headspace during sampling and the assumption of a linear increase/decrease in gas concentration with time (Chadwick et al., 2014; Christiansen et al., 2011; Denmead, 2008). Through time, different guidelines have been proposed to advance the standardisation of static chamber techniques (de Klein et al., 2015; Pavelka et al., 2018; Rochette, 2011) but essentially the basic method has remained unchanged for decades (Chadwick et al., 2014; Hutchinson and Mosier, 1981).

Alternative approaches to the static chamber method include the use of (semi-) automated chambers and micrometeorological techniques that allow $F_{\text{N}_2\text{O}}$ measurements at higher temporal frequency and resolution (Baldocchi, 2014; Pavelka et al., 2018; Rapson and Dacres, 2014). Recent developments in the technology of fast-response analysers have enabled e.g. tunable diode laser absorption spectrometers, Fourier transform infrared spectrometers and, in particular, continuous-wave quantum cascade laser absorption spectrometers (QCL) to be coupled to automated chambers (Brümmer et al., 2017; Cowan et al., 2014; Savage et al., 2014) or eddy covariance (EC) systems (Nemitz et al., 2018; Nicolini et al., 2013). Despite these recent advances in analyser technology, our understanding of the micro- and macro-scale processes that lead to the emission of N_2O has remained limited. While chamber measurements help to examine the interaction between soil processes and $F_{\text{N}_2\text{O}}$ at point scales, EC promotes the understanding of diurnal, seasonal and annual $F_{\text{N}_2\text{O}}$ dynamics at field to ecosystem scale (Cowan et al., 2020;



Liáng et al., 2018; Luo et al., 2017). Some studies have aligned chamber and EC measurements to determine the full range of processes that drive F_{N_2O} dynamics across these different scales but still relied on the use of more than one analyser for measuring F_{N_2O} (Jones et al., 2011; Tallec et al., 2019; Wecking et al., 2020a).

In this study, we tested whether a single field-deployed QCL could be used for manual injections of gas samples taken from static chambers to allow nearly concurrent measurements of chamber N_2O samples alongside continuous EC. Field measurements using a QCL system for both these purposes have, to our knowledge, not yet been conducted. Our objective was to examine whether chamber F_{N_2O} determined by field-based QCL ($F_{N_2O_QCL}$) were equivalent to F_{N_2O} determined by laboratory GC ($F_{N_2O_GC}$). Orthogonal regression analysis was used to quantify the correlation between $F_{N_2O_QCL}$ and $F_{N_2O_GC}$. However, as correlation studies include limitations when assessing the comparability between two methods (i.e. GC and QCL), we also conducted Bland Altman and bioequivalence analyses to determine the degree to which N_2O concentrations and fluxes derived from QCL would be comparable to GC.

2 Methods

2.1 Study site

This study was conducted at Troughton Farm, a commercially operating 199 ha dairy farm in the Waikato region, 3 km east of Waharoa (37.78°S, 175.80°E, 54 m a.s.l.), North Island, New Zealand. The farm had been under long-term grazing for at least 80 years with micrometeorological measurements using a QCL EC system made since November 2016 (Liáng et al., 2018; Wecking et al., 2020a). Mean annual temperature and precipitation, recorded at a climate station 13 km to the south-west of the farm (1981–2010), were 13.3 °C and 1249 mm, respectively (NIWA, 2018). The experimental site comprised three paddocks (P51, P53, P54) in the north of the farm with each sized about 2.8 ha. Soils were formed in rhyolitic and andesitic volcanic ash and rhyolitic alluvium. The dominant soil type based on the New Zealand soil taxonomy was a Mottled Orthic Allophanic soil (Te Puinga silt loam) (Hewitt, 2010). Plots used for the static chamber measurement of this study were located on P53 around 50 m to the south-west of the EC system.

2.2 Experiment design

One intensive field campaign was conducted between 10 and 16 September 2019. The campaign's primary purpose was to 1) manually collect gas samples from static chambers comprising potentially low to high N_2O concentrations (C_{N_2O}); 2) analyse these samples on-site using QCL and off-site using GC; 3) to quantify and compare resulting C_{N_2O} and F_{N_2O} . A thorough description of the QCL operating in EC mode has been provided by Liáng et al. (2018) and Wecking et al. (2020a).

2.2.1 Static chamber measurements

The static chamber trial comprised a randomised block design of circular treatment and control plots each of which included three replicates per treatment/control. Ammonium nitrate (AN) fertiliser was used as a treatment and applied at different rates



to ensure production of a wide range of F_{N_2O} for subsequent flux measurements. The three applications rates were 300 (AN_{300}), 600 (AN_{600}) and 900 kg N ha⁻¹ (AN_{900}), while the control plots (AN_0) did not receive any AN. Separate areas adjacent to the twelve chamber plots were established to collect soil samples for laboratory analyses of soil moisture and soil mineral nitrogen (N_{min}). Soil moisture and water-filled pore space (WFPS) were analysed and calculated using the methods described in Wecking et al. (2020a). Soil N_{min} was derived from field-moist soil samples extracted in 2M KCl (Mulvaney, 1996) and measured colorimetrically using a Skalar SAN++ flow analyser (Skalar Analytical B. V., Breda, Netherlands). Both, NH_4^+ and NO_3^- , were expressed in units kg ha⁻¹ using a site-specific soil dry bulk density of 0.73 g cm⁻³ (Wecking et al., 2020a).

Flux measurements were made on the day of treatment application and throughout the following six days with chamber gas samples collected on nine occasions (Table S1). The sampling followed a standardised chamber technique (de Klein et al., 2003; de Klein et al., 2015; Luo et al., 2008b) and was carried out daily at 10 AM (NZDT) (van der Weerden et al., 2013). Additional sampling was conducted at noon on 12 and 15 September. Before sampling, PVC lids were fitted to water-filled base channels that provided a gas-tight seal over the 10 L headspace of the chambers. Gas samples were taken from this headspace during a 45 min enclosure period at four times – t_0 , t_{15} , t_{30} and t_{45} – per chamber (Pavelka et al., 2018). A sampling port served to extract air from the chamber headspace by using a 60 mL plastic syringe (Terumo Corp., Tokyo, Japan). After flushing the syringe three times with air from the chamber headspace, the following procedure was applied to ensure that GC and QCL analysis received identical headspace samples: 1) after flushing, 60 mL of sample air was extracted from the chamber headspace; 2) 10 mL of the sample was discarded to flush the syringe needle; 3) 15 mL was transferred into a pre-evacuated, septum-sealed, screw-capped 5.6 mL glass vial (Exetainer, Labco Ltd., High Wycombe, UK); 4) the syringe needle was flushed again by discarding a further 10 mL; and 5) a second pre-evacuated glass vial was over-pressurised with 15 mL, and the remainder discarded. The procedure was repeated for each sample resulting in a total of 2 x 432 samples, i.e. two replicated sample batches for subsequent GC (1 x 432 samples) and QCL (1 x 432 samples) analyses.

2.2.2 Laboratory gas chromatography

Gas chromatography was conducted on the first sample batch at the New Zealand National Centre for Nitrous Oxide Measurements (NZ-NCNM) at Lincoln University, New Zealand. Automated analysis (GX-271 Liquid Handler, Gilson Inc., Middleton, WI) was performed using a SRI 8610 GC (SRI Instruments, Torrance, CA, USA) and a Shimadzu GC-17a (Shimadzu Corp., Kyoto, Japan) equipped with a ⁶³Ni-electron capture detector. The analysis followed standard procedures described in detail by de Klein et al. (2015). Oxygen-free, ultra high purity nitrogen (N_2) was used as the carrier gas (mobile phase) at a flow rate of 0.4 L min⁻¹. The measurement frequency was set to 1 Hz. Sample exetainers experienced a storage time of up to two weeks prior to their analysis which was due to transportation from the field site to the laboratory. The run time during GC analysis was about eight minutes per sample.



2.2.3 Field quantum cascade laser absorption spectrometry

The second batch of N₂O samples was analysed immediately after chamber sampling by manual injection into a continuous-wave quantum cascade laser absorption spectrometer (QCL, Aerodyne Research Inc., Billerica, MA, USA). Briefly, QCL uses infrared (IR) light energy which is passed through a 0.5 L multiple pass absorption cell with a pathlength of 76 m. Inside the cell, N₂O absorbs IR light energy which then is quantified as equivalent to the compositional N₂O concentration of the gas sample measured (Nelson et al., 2004).

For the purpose of our analysis, we switched the QCL from its continuous measurement (EC) mode to an ‘injection mode’. The injection mode conversion took less than 30 minutes: a stainless steel three-way valve (Swagelok, Solon, OH, USA) mounted to the air inlet of the QCL allowed re-direction of the air flow from the primary inlet tube of the EC system into a second, 1 m long Bev-A-line tube (4 mm internal diameter). At its end, the tube was connected to a pressure regulator and a bottle of oxygen free, industrial grade N₂ carrier gas (BOC Ltd., NZ). Two stainless steel, T-junction connectors (Swagelok, Solon, OH, USA) were fitted to the sample tube allowing overflow of excess carrier gas through a 0.45 µm PTFE membrane filter (ThermoFisher, Scientific, NZ) and sample injection through a septum-sealed port (Fig. 1). A dry scroll vacuum pump (XDS35i, Edwards, West Sussex, UK) was used for both EC measurements and manual injections to continuously draw either air or carrier gas through the QCL sample cell.

Once the injection line had been established, the flow rate was reduced from an initial 15 L min⁻¹ used for EC to 1 L min⁻¹ for manual injections, based on Lebegue et al. (2016), Savage et al. (2014) and Brümmer et al. (2017). The reduction in flow was monitored using a RMA-SSV flow meter (Dwyer Instruments, PTY. Ltd., Michigan City, IN, USA) while setting the inlet control valve of the QCL to 2 V (using the TDLWintel software command) before manually adjusting inlet and outlet control valves of the QCL device further until the desired flow rate was achieved. Prior to sample injection, a minimum lag time of ten minutes was applied to let temperature and pressure of the QCL and its temperature-controlled enclosure box return to steady-state, i.e. 35 ± 0.5 Torr, 33.5 °C laser temperature and QCL enclosure box temperature of 30 ± 0.1 °C.

Standards of certified N₂O concentration (range 0.2 to 100 ppm) were injected before, during and after each sample run and complemented QCL analysis (Table S2). Ten out of the twelve N₂O standards were provided by the NZ-NCNM (except 0.321 and 0.401 ppm) and, therefore, were identical to those used for GC (Sect. 2.2.2). The QCL measurements were made at 10 Hz frequency with 1 mL of sample air extracted from each sample exetainer and manually injected into the flow of N₂ carrier gas by using a glass syringe (SGE International PTY Ltd., VIC, Australia). The glass syringe was flushed with N₂ gas after each injection to avoid cross-contamination of samples or N₂O standards. Generally, using a 1 mL glass syringe was preferred to commonly used insulin syringes because of its higher accuracy resulting in greater output peak areas (Fig. S1c). The selection of syringe type, flow rate and the usage of N₂O standards were based on preliminary tests conducted in advance of the actual field campaign (Fig. S1).



2.3 Data processing

Using GC and QCL resulted in the raw output of peak area data from injected N₂O standards and chamber derived N₂O samples. To compute final C_{N2O}, peak area data from N₂O standards were fitted to linear and quadratic (second-order-polynomial) models (de Klein et al., 2015; van der Laan et al., 2009). Whereas de Klein et al. (2015) recommended the use of quadratic curves models for data measured by GC analysis, we found that both linear and quadratic models adequately fitted sample data derived from QCL. Using a linear fit ultimately resulted in on average 3 % smaller F_{N2O_QCL} (range -0.5 % to -4.3 %) than using a quadratic model. Nonetheless, since the quadratic fit suited lower C_{N2O} better than a linear fit, quadratic models were preferred when generated from standards of known N₂O concentration (Fig. S1a, b). The actual quadratic model used to calculate final C_{N2O} of the gas samples was based on a selection of standards fitted to the expected minimum and maximum range of real sample C_{N2O}; which in our study did not exceed 10 ppm. Output data from GC were processed in PeakSimple software (SRI Instruments, Torrance, CA, USA) and Excel (Microsoft Corp. Redmond, WA, USA). MATLAB R2017a scripting (MathWorks Inc., Natick, MA, USA) was used for data derived from the QCL.

2.4 Flux calculation

The N₂O flux in mg N₂O-N m⁻² hr⁻¹ was calculated for both data streams, GC (F_{N2O_GC}, n = 108) and QCL (F_{N2O_QCL}, n = 108), by applying a linear regression function to the increase in chamber headspace C_{N2O} between time t₀ and t₄₅ following Eq (1) (van der Weerden et al., 2011):

$$F_{N2O_GC} \text{ and } F_{N2O_QCL} = \frac{\Delta N_2O}{\Delta T} \times \frac{M}{V_m} \times \frac{V}{A} \quad (1)$$

where ΔN₂O is the increase in headspace C_{N2O} (μL N₂O L⁻¹ (ppmv)) over time; ΔT is the enclosure period (in hours); M is the molar weight of nitrogen in N₂O (44 g mol⁻¹); V_m is the molar volume of gas (L mol⁻¹) at the mean air temperature recorded at each sampling occasion; V is the chamber headspace volume (m³); and A is the area covered by the chamber base, here 0.0415 m². All F_{N2O} were converted to units of nmol N₂O m⁻² s⁻¹. The integration of F_{N2O_GC} (n = 84) and F_{N2O_QCL} (n = 84) determined at 10 AM sampling was used to quantify the proportion of applied nitrogen emitted as N₂O (E_{N2O}) across the seven day trial in units kg N₂O-N ha⁻¹ based on Luo et al. (2007) and Wecking et al. (2020a).

2.5 Statistical analyses

The statistical analysis for C_{N2O} data (C_{N2O_GC} and C_{N2O_QCL}, each n = 432) and resulting F_{N2O} (F_{N2O_GC} and F_{N2O_QCL}, each n = 108) was conducted in Genstat® (Version 19, VSN International, Hemel Hempstead, UK). After testing for normality using a Shapiro-Wilk test and homogeneity of variance by examining residual and fitted values, we applied three different statistical approaches to compare GC with QCL data: 1) orthogonal regression, 2) Bland Altman and 3) bioequivalence statistics.

The orthogonal regression analysis used standardised C_{N2O} and F_{N2O} data following Eq (2):

$$\text{standardised } C_{N2O} \text{ and } F_{N2O} = \frac{(x - \text{mean})}{\text{standard deviation}} \quad (2)$$



The core of this orthogonal regression was a principal component analysis which, in contrast to ordinary least square regression, allowed for measurements errors in both the response and the predictor variable by minimising the squared residuals in vertical and horizontal direction. While orthogonal regression returned a Pearson correlation coefficient r that provided information about the strength of the linear relationship between GC and QCL data, we found that r did not include any predication about the level of agreement between the two methods (Bland and Altman, 1986; Giavarina, 2015). The degree to which GC and QCL data would agree was, for that reason, determined by using Bland Altman statistics that quantified the bias (i.e. the mean difference) and the limits of agreement between the two methods. The limits of agreement were calculated from the mean and the standard deviation (SD) of the difference between GC and QCL data. We defined that 95 % of all data points had to be within ± 1.96 SD of the mean difference (Giavarina, 2015). The Bland Altman analysis was conducted for individual $F_{N_{2O}}$ as well as for mean $F_{N_{2O}}$ across replicates of the same treatment.

Still, testing for correlation and agreement did not determine whether GC and QCL data would effectively and for practical purposes be the same (termed ‘bioequivalent’). We, therefore, used bioequivalence statistics to assess the biological and analytical relevance of the difference between the two methods. The first part of this analysis comprised an one-way analysis of variance (ANOVA) for $F_{N_{2O}}$ which was subset by treatment (AN_0 , AN_{300} , AN_{600} , AN_{900}) and analytical device (GC, QCL). Results from this ANOVA determined the 90 % confidence intervals (CI) of the mean difference between $F_{N_{2O_QCL}}$ and $F_{N_{2O_GC}}$. In bioequivalence statistics, the 90 % CI (corresponding to 80 % power) is generally preferred instead of using a 95 % CI that often serves to establish a statistical difference between two methods or treatments rather than proving no difference. An important component of the analysis was to also define the bioequivalence range, i.e. the maximum acceptable difference, between the new (QCL) and the standard method (GC). Bioequivalence statistics acknowledge that two methods will never be exactly the same. Defining an acceptable bioequivalence range is, thus, an important precondition and might in some cases be even provided by a regulatory authority. While commonly used in pharmaceutical research (Bland and Altman, 1986; Giavarina, 2015; Patterson and Jones, 2006; Rani and Pargal, 2004), the concept of bioequivalence has not broadly been applied in environmental sciences. Therefore, an acceptable bioequivalence range for N_2O data based on the use of different analysers and methods has yet to be defined. We determined that the maximum acceptable difference of $F_{N_{2O_QCL}}$ in our study had to be as small as possible and within ± 5 % of the mean difference of the standard method ($F_{N_{2O_GC}}$). The null hypothesis ($F_{N_{2O_QCL}}$ is different from $F_{N_{2O_GC}}$) was rejected when the 90 % CI of the difference ($F_{N_{2O_QCL}} - F_{N_{2O_GC}}$) was entirely within the predefined bioequivalence range at a significance level of 5 %. Following the same principles, we conducted a bioequivalence analysis for $C_{N_{2O_QCL}}$ and $C_{N_{2O_GC}}$.

3 Results and discussion

3.1 Environmental conditions and soil variables

Daily mean air temperatures during the seven-day chamber campaign ranged from 8.3 to 12.8 °C. The WFPS of chamber and associated soil plots did not fall below 73.9 % with a mean of 79.5 %. Cumulative rainfall for September 2019 was 119 mm



220 compared to only 2 mm occurring during the seven days of the campaign. As expected, soil NH_4^+ and NO_3^- levels increased with increasing application of AN fertiliser. The highest values of N_{\min} measured at AN_{900} plots were 265 kg NH_4^+ ha $^{-1}$ and 268 kg NO_3^- ha $^{-1}$. The mean background levels of soil NH_4^+ and NO_3^- were around 2 kg ha $^{-1}$. At the end of the campaign, soil NH_4^+ levels for all treatments had decreased by less than half while the amount of soil NO_3^- remained similar to the initial level measured on the day of treatment application (Table S3).

225 3.2 Comparing GC and QCL derived data

3.2.1 Magnitude and general variability

Measurements resulted in a wide range of $F_{\text{N}_2\text{O}}$ but followed the same temporal and treatment-dependent patterns for both $F_{\text{N}_2\text{O_GC}}$ and $F_{\text{N}_2\text{O_QCL}}$. The magnitude of individual fluxes was between -0.10 and 22.24 nmol $\text{N}_2\text{O m}^{-2} \text{s}^{-1}$ for $F_{\text{N}_2\text{O_GC}}$ and -0.07 and 22.81 nmol $\text{N}_2\text{O m}^{-2} \text{s}^{-1}$ for $F_{\text{N}_2\text{O_QCL}}$. The mean $F_{\text{N}_2\text{O}}$ ($n = 27$) from chamber plots that received the highest application rate of AN fertiliser (AN_{900}) was 13.22 nmol $\text{N}_2\text{O m}^{-2} \text{s}^{-1} \pm 1.47$ (\pm standard error of the mean, SEM) for $F_{\text{N}_2\text{O_GC}}$ and 13.27 nmol $\text{N}_2\text{O m}^{-2} \text{s}^{-1} \pm 1.43$ for $F_{\text{N}_2\text{O_QCL}}$. Similarly, the AN_{600} treatment had a mean $F_{\text{N}_2\text{O}}$ of 8.51 nmol $\text{N}_2\text{O m}^{-2} \text{s}^{-1} \pm 0.98$ ($F_{\text{N}_2\text{O_GC}}$) and 8.33 nmol $\text{N}_2\text{O m}^{-2} \text{s}^{-1} \pm 0.9$ ($F_{\text{N}_2\text{O_QCL}}$). The mean $F_{\text{N}_2\text{O}}$ for AN_{300} was 6.61 nmol $\text{N}_2\text{O m}^{-2} \text{s}^{-1} \pm 0.78$ ($F_{\text{N}_2\text{O_GC}}$) and 6.48 nmol $\text{N}_2\text{O m}^{-2} \text{s}^{-1} \pm 0.69$ ($F_{\text{N}_2\text{O_QCL}}$). At control plots, $F_{\text{N}_2\text{O}}$ were close to zero (Fig 2; Table S3). We found that treatment $F_{\text{N}_2\text{O}}$ increased from a near zero background flux to ≥ 8.5 nmol $\text{N}_2\text{O m}^{-2} \text{s}^{-1}$ on the second day of the campaign. From then, AN_{300} fluxes gradually decreased with time whereas $F_{\text{N}_2\text{O}}$ for AN_{600} and AN_{900} remained relatively elevated until the last day of the trial (Fig. 2). These temporal trends align with Cowan et al. (2020) who observed N_2O emissions to peak within seven days after urea and AN fertiliser application; and found that $F_{\text{N}_2\text{O}}$ returned to background levels after two or three weeks. Similarly, short-term responses of $F_{\text{N}_2\text{O}}$ to AN application were also determined by others, e.g. Bouwman et al. (2002); Jones et al. (2007) and Cardenas et al. (2019). However, for our study AN treatment effects on $F_{\text{N}_2\text{O}}$ were of secondary interest.

240 Different rates of AN fertiliser were only applied to result in a wide range of $F_{\text{N}_2\text{O}}$ (low to high) and thereby to allow for a methodological comparison of GC and QCL data.

3.2.2 AN treatment flux and concentration data

The correlation between calculated $F_{\text{N}_2\text{O_GC}}$ and $F_{\text{N}_2\text{O_QCL}}$ and between $C_{\text{N}_2\text{O_GC}}$ and $C_{\text{N}_2\text{O_QCL}}$ across all treatments was high with an r value of 0.996 resulting from orthogonal regression (Fig. 3a, 3b). For both cases, major axis, ordinary and inverse least squares were nearly identical to a 1:1 line. All three regression models could therefore be used similarly well to predict the strength of the linear relationship between $F_{\text{N}_2\text{O_GC}}$ and $F_{\text{N}_2\text{O_QCL}}$ and $C_{\text{N}_2\text{O_GC}}$ and $C_{\text{N}_2\text{O_QCL}}$, respectively (Table S4). The results of the orthogonal regression analysis suggested that QCL delivered equivalent data to the GC method. The Bland Altman statistic quantified a percentage difference between the two methods for $F_{\text{N}_2\text{O}}$ (i.e. $F_{\text{N}_2\text{O_GC}}$ and $F_{\text{N}_2\text{O_QCL}}$ treatment means) of not smaller than -11.2 % and not greater than +9.2 % (Table S5). The percentage difference between individual $F_{\text{N}_2\text{O_GC}}$ and $F_{\text{N}_2\text{O_QCL}}$ (not treatment means) was slightly greater but in only less than 3 % of all cases exceeded +10 % and -15



%, which was likely due to the higher variability of F_{N_2O} between individual replicates of the same treatment. For both cases, $\geq 95\%$ of all data points were well within the pre-defined limits of agreement ± 1.96 SD (Fig. 4b). The overall mean difference (bias) between $F_{N_2O_GC}$ and $F_{N_2O_QCL}$ was $0.1 \text{ nmol N}_2\text{O m}^{-2} \text{ s}^{-1}$ (Fig. 4b). However, this small bias might be practically irrelevant when compared with the overall detection limit of static chambers and other general uncertainties. Neftel et al. (2007), for instance, quantified a chamber detection limit of $0.23 \text{ nmol N}_2\text{O m}^{-2} \text{ s}^{-1}$ whereas Parkin et al. (2012) reported $0.03 \text{ nmol N}_2\text{O m}^{-2} \text{ s}^{-1}$. At the annual scale, Flechard et al. (2007) and others (e.g. Jones et al., 2011; Rochette and Eriksen-Hamel, 2008) showed that the uncertainty of integrated fluxes can be as high as 50 % when using the static chamber method.

3.2.3 Control flux and concentration data

In contrast to the strong comparability of GC and QCL data at AN treatment sites, $F_{N_2O_GC}$ and $F_{N_2O_QCL}$ measured at control plots (AN_0) were only poorly correlated ($r = 0.3064$) (Fig. 3c). The model-fit of major axis, ordinary and inverse least squares indicated that the regression of $F_{N_2O_GC}$ on $F_{N_2O_QCL}$ (and vice versa) was not identical, i.e. differed in the minimisation of squared residuals in vertical and horizontal direction. Likewise, this also applied to $C_{N_2O_GC}$ and $C_{N_2O_QCL}$ (Fig. 3d). Mean F_{N_2O} ranged from a minimum of -0.05 to a maximum of only $0.21 \text{ nmol N}_2\text{O m}^{-2} \text{ s}^{-1}$ (Table S3). Consequently, Bland Altman statistics determined only small quantitative differences between $F_{N_2O_GC}$ and $F_{N_2O_QCL}$. When computing the percentage difference between these $F_{N_2O_GC}$ and $F_{N_2O_QCL}$, we found near-zero F_{N_2O} from AN_0 plots were less consistent in relative terms than treatment F_{N_2O} (Fig. 4, Table S5). However, these inconsistencies were generally small and did not appear of great biological interest.

More generally, QCL analysis resulted in slightly higher C_{N_2O} than GC, which might explain why the calculated $F_{N_2O_QCL}$ at AN_0 plots were higher than $F_{N_2O_GC}$ (Table S5). However, whether this finding was related to the potentially higher sensitivity of the QCL device or due to other possible variations in sampling procedures was not resolved. Instead, we found that the disagreement between the GC and QCL method was likely related to ambient N_2O concentrations in the chamber headspace that remained between 300-400 ppb and showed a non-linear response with time, regardless of which analytic device was used. This might have resulted in the calculation of very small but apparent positive and negative F_{N_2O} , when in fact the actual flux was zero (*Type I error* as defined by Parkin et al. (2012)). The integration of C_{N_2O} with time to calculate F_{N_2O} , therefore, likely included this error; rather than being caused by uncertainties associated with measurement procedures or analytic device (Kroon et al., 2008). Hence, the deviation of F_{N_2O} determined at control sites (AN_0) from treatment F_{N_2O} (AN_{300} , AN_{600} , AN_{900}) has to be taken into account when evaluating the above results and mathematical principles (Sect. 3.2.2). Since static chamber measurements often include near-ambient C_{N_2O} and F_{N_2O} equal or near-zero, F_{N_2O} from control plots were kept in the manuscript for the purpose of completeness.

3.2.4 Cumulative N_2O emissions

Cumulative N_2O emissions across the seven-day campaign were quantified slightly greater for the GC ($E_{N_2O_GC}$) than the QCL ($E_{N_2O_QCL}$) method. The mean difference between $E_{N_2O_GC}$ and $E_{N_2O_QCL}$ for the control (AN_0) and each treatment, AN_{300} , AN_{600}



and AN_{900} , was -0.011 , $+0.0023$, $+0.050$ and $+0.028 \text{ kg N ha}^{-1}$, respectively. This was a difference of less than 4 % in total N_2O emissions during deployment (Fig. 5).

3.3 Measurement performance of QCL analysis

The measurement precision of QCL, and particularly GC, have been generally well-reviewed (de Klein et al., 2015; Lebegue et al., 2016; Rapson and Dacres, 2014). The precision of common GC analysers is $< 0.5 \text{ ppb}$ (Rapson and Dacres, 2014; van der Laan et al., 2009) while the precision of QCL was found to be about 0.3 ppb for measurements made at 10 Hz and 0.05 ppb for 1 Hz ; but in some cases might be even higher ($\sim 1 \text{ ppt}$) (Curl et al., 2010; Rapson and Dacres, 2014; Savage et al., 2014). Zellweger et al. (2019), for instance, used laboratory QCL for the calibration of N_2O reference standards to inform the internationally accepted calibration scale of the Global Atmosphere Watch Programme of the World Meteorological Organisation. Similarly, Rosenstock et al. (2013) preferred lab-based QCL to verify the accuracy and precision of different photoacoustic spectrometers.

However, the analytic precision was also found to depend on factors other than the technical performance of the analytic device. Rannik et al. (2015) indicated that the performance (and thus the precision of $\text{F}_{\text{N}_2\text{O}}$) of an analyser to measure static chamber derived gas samples is likely more limited by the precision of the chamber system than by errors related to analysis or post-processing of the data itself. Imprecisions might be caused by several factors, e.g. chamber type and dimension, experimental set-up, deployment time and preferred sampling method, all of which would lead to differences in the flux detection limit (Sect. 3.2.2). In contrast, the sources of uncertainty in our study were most likely related to: 1) insufficient evacuation of glass exetainers leading to the sporadic dilution of gas samples and N_2O standards; and 2) variation of sample volume when injected into the QCL, which might not have been equal to 1 mL in practice and, thus, could have resulted in slight variations of output peak area. In agreement with these observations, de Klein et al. (2015) found that half the measurement uncertainty could be explained by the variability of gas sample volume in the sample exetainers. The inclusion of a fixed volume sample loop when injecting gas samples into the QCL might help to reduce this source of error.

As the N_2O analysis using QCL was conducted in a temperature and pressure controlled environment, variations in these parameters were unlikely. The temperature dependency of N_2O analysis by QCL was described as being linear by Lebegue et al. (2016) with variations less than $0.02 \text{ ppb } ^\circ\text{C}^{-1}$. To reduce the uncertainty of output peak area, we recommend a constant baseline flow of N_2 carrier gas at constant pressure (slightly higher than ambient) and temperature for manual injections made into the QCL device. Depending on the set-up of the QCL system, an initial lag time of 10 to 30 min before injections might be required to ensure sufficient stabilisation of pressure and temperature in the QCL sample cell. Given a flow rate of 1 L min^{-1} , the delay between single injections of 1 mL sample volumes was short (5 to 8 sec). Sample concentrations at the same volume but $> 20 \text{ ppm}$ N_2O required a longer delay time between individual injections ($> 20 \text{ sec}$) to enable sufficient flushing of the QCL sample cell and to avoid cross-contamination. The identification of suitable delay times was straight forward and could be accessed easily in real time by visually examining the peak progression in TDLWintel. However, we did not determine the extend to which spontaneous but small variations in the flow rate of N_2 carrier gas would have affected the resulting output



peak areas. Further uncertainties of true output peak areas might have also been associated with processing and curve fitting procedures applied to the raw dataset in MATLAB that likely led to small underestimations.

3.4 QCL injections

3.4.1 The concept of bioequivalence

320 Using the Pearson correlation coefficient and the coefficient of determination for comparing two or more quantitative methods is a generally preferred approach in the field of N₂O research. Comparisons of different methods for N₂O analysis made in the literature most commonly used orthogonal (Jones et al., 2011) and linear regression (Brümmer et al., 2017; Cowan et al., 2014; Tallec et al., 2019), Students t-tests (Christiansen et al., 2015) or were based on raw data (Savage et al., 2014). However, correlation studies as such have limitations when assessing the comparability between two methods since a correlation analysis
 325 only identifies the relationship between two variables, not the difference (Giavarina, 2015). Bland Altman and bioequivalence statistics overcome this limitation by assessing the degree of agreement between methods.

An important aspect of statistical hypothesis testing is that the null hypothesis is never accepted. But failure to reject the null hypothesis is not the same as proving no difference. A bioequivalence assessment allows the statistical assessment of whether two methods (e.g. measurement devices, drug treatment) are effectively the same. Central to a bioequivalence analysis is the
 330 “equivalence range” that defines the size of the acceptable difference for which the values are similar enough to be considered equivalent. This becomes important when considering that even with the most precise analytical design and the most tightly controlled experimental conditions, e.g. F_{N2O_GC} and F_{N2O_QCL} will never be exactly the same (Rani and Pargal, 2004). However, if the difference is sufficiently small for ‘practical purposes’, F_{N2O_GC} and F_{N2O_QCL} can be considered effectively the same. Here, an accepted proof of bioequivalence for F_{N2O_QCL} was if the 90 % confidence interval of the difference F_{N2O_QCL}-F_{N2O_GC}
 335 (corresponding to a test with size 0.05) was within a ± 5 % difference of F_{N2O_GC}.

The accepted proof of bioequivalence can vary depending on the objective of the research or guidelines provided by a regulatory authority but commonly does not exceed ± 20 % (Rani and Pargal, 2004; Ring et al., 2019; Westlake, 1988). In our study, a small bioequivalence range of ± 5 % was preferred to test the difference between F_{N2O_QCL} and F_{N2O_GC} since such recommendations did not exist.

340 Overall, our results showed that F_{N2O_GC} and F_{N2O_QCL} from AN₃₀₀, AN₆₀₀ and AN₉₀₀ plots met the criterion for bioequivalence. The 90 % confidence intervals of the difference (F_{N2O_GC}-F_{N2O_QCL}) were quantified 0.127 (AN₃₀₀), 0.185 (AN₆₀₀) and -0.043 (AN₉₀₀) nmol N₂O m⁻² s⁻¹ and well within the pre-defined equivalence range of ± 5 % (Fig. 6e, Table S 6). At control sites (AN₀), F_{N2O_GC} and F_{N2O_QCL} did not meet the criterion for bioequivalence. However, the failure to establish bioequivalence for AN₀ sites was due to the overall limitation of the static chamber method to provide ‘real’ F_{N2O}; rather than based on failure
 345 of the statistical principle (Sect. 3.2.3). On the contrary, when tested for C_{N2O} instead of F_{N2O}, bioequivalence was confirmed for t₀ and t₁₅ but did not apply for t₃₀ and t₄₅ (Fig. 6a). Again, failure to establish bioequivalence was likely related to limitations of the static chamber method that, in this case, was indicated by the lower boundary of the 90 % CI remaining outside the



predefined bioequivalence ranges. Another possible reason for failing to establish bioequivalence for GC and QCL derived data at AN₀ sites could have been the maximum acceptable difference between the two methods itself. We defined (Sect. 2.5) that this difference had to be within $\pm 5\%$ of the mean difference of the standard method (i.e. GC). However, it has to be taken into consideration that the accepted proof of bioequivalence would have led to different results if the percentage mean difference had been set to, for instance, $\pm 10\%$. Consequently, accepting a greater mean difference between the two methods would have resulted in determining bioequivalence for C_{N₂O}_GC and C_{N₂O}_QCL even at ambient concentration. More generally, we found that positive values of the 90 % CI of the difference indicated that the difference between the two methods (GC-QCL) resulted in higher C_{N₂O}_GC and F_{N₂O}_GC. Negative values, instead, showed that the difference GC-QCL led C_{N₂O}_QCL and F_{N₂O}_QCL to be higher than C_{N₂O}_GC and F_{N₂O}_GC. The overall difference between the two methods did not exceed ± 0.1 ppm for C_{N₂O} and ± 0.38 nmol N₂O m⁻² s⁻¹ for F_{N₂O} (Fig. 6e).

To the best of our knowledge, bioequivalence has not broadly been applied in the greenhouse gas literature to identify and to discuss the range at which a difference in F_{N₂O}_GC and F_{N₂O}_QCL could be considered relevant when using different analytical methods. Defining the magnitude of F_{N₂O} (e.g. in nmol N₂O m⁻² s⁻¹) at which a unit difference would actually become relevant, however, is important when using different methods to quantify, compare and ultimately upscale N₂O emissions. We, therefore, recommend bioequivalence or other statistical approaches (e.g. Bland Altman) for more formally assessing the agreement between two methods in the future.

3.4.2 Strengths and weaknesses

The employment of a QCL analyser offers an alternative approach for the injection of N₂O samples taken from static chambers, particularly as F_{N₂O}_QCL were generally bioequivalent to F_{N₂O}_GC. Using a QCL for the purpose of manual injections can be conducted without much disruption to other measurements (e.g. EC or automated chambers) and, therefore, helps justify the initially higher capital and general running costs involved with operating a QCL device. Additional labour effort and time associated with sample storage and transport necessary for laboratory GC do not necessarily apply for field-based injections into a QCL. Once established, a QCL system has relatively low maintenance and offers a straightforward application for manual injections in addition to EC or other measurements. In our study, the assembly of the injection set-up required little equipment and was installed within 30 min. This allowed for a rapid analysis after chamber sampling without greatly interfering with other measurements, such as EC, that were offline during the time of manual injection into the QCL.

We acknowledge that sporadic dilution of N₂O samples might have occurred for both GC and QCL analyses due to sample storage in and insufficient evacuation of sample exetainers (de Klein et al., 2015). Despite this potential source of uncertainty, storing N₂O samples in exetainers enabled repeated injections from the same sample for multiple times and also allowed sample injections at suitable times, i.e. postponing analysis if EC measurements were of higher importance or if weather conditions (e.g. precipitation) did not support manual injections into the QCL (Faust and Liebig, 2018). Similar to GC, QCL injections required consumables (N₂ carrier gas and N₂O standards) but, in contrast, time and costs associated with laboratory work were substantially less (Table 1).



4 Conclusion

Previously, QCL had been used either in conjunction with EC or coupled to automated chambers. Here, we showed that one QCL device could be used as a tool for the analysis of static chamber derived N_2O samples without major disruption to these other measurement tasks. We found treatment N_2O concentrations ($C_{\text{N}_2\text{O_QCL}}$) and fluxes ($F_{\text{N}_2\text{O_QCL}}$) from QCL were in agreement with results based on laboratory GC ($C_{\text{N}_2\text{O_GC}}$, $F_{\text{N}_2\text{O_GC}}$). The percentage difference between treatment $F_{\text{N}_2\text{O_GC}}$ and $F_{\text{N}_2\text{O_QCL}}$ was not smaller than -11.2 % and not greater than +9.2 % with a mean difference between the two of only 0.1 $\text{nmol N}_2\text{O m}^{-2} \text{ s}^{-1}$. Deviation between the GC and QCL methods was determined only for close to zero $F_{\text{N}_2\text{O}}$ at control plots where $F_{\text{N}_2\text{O_GC}}$ and $F_{\text{N}_2\text{O_QCL}}$ values were found outside the predefined bioequivalence range. However, this was likely due to the calculation of very small but apparent positive and negative $F_{\text{N}_2\text{O}}$ when in fact the actual flux was zero; rather than being caused by uncertainties related to GC or QCL analysis itself. Bioequivalence was determined for all other $F_{\text{N}_2\text{O_GC}}$ and $F_{\text{N}_2\text{O_QCL}}$, i.e. it was confirmed that GC and QCL data were for practical purposes the same. We found that using Bland Altman and bioequivalence statistics in addition to regression analysis served the comparison of GC and QCL particularly well. Yet, these two statistical approaches have not been broadly used in the field of greenhouse gas research to compare different analytical methods or to discuss the magnitude at which a difference in $F_{\text{N}_2\text{O}}$, or other greenhouse gas fluxes, would become relevant. Since correlation studies identify the relationship between two methods but not the difference, we recommend that bioequivalence or other suitable statistical approaches are used for more formally assessing the agreement between two methods. Finally, QCL offers a great potential to interlink different methods of gas measurements across different temporal and spatial scales. In the future this capability might not only be important for measuring N_2O but equally also applies to the measurement of other gas species (e.g. CO_2 , CH_4) and gas isotopomers of interest.

Data availability

Data were deposited at the University of Waikato Research Commons, see (Wecking et al., 2020b) <https://researchcommons.waikato.ac.nz/handle/10289/13539>

Supplements to this manuscript exist.

Author contributions

ARW, VC, JL and LS designed the experiment. ARW performed the field work. ARW conducted the post-processing of GC and QCL data using MATLAB scripts provided by AW and DC. ARW performed the statistical analysis with inputs and contributions from VC. VC and LS commented on the results of the initial data analysis. ARW wrote and revised the manuscript with contributions from VC, AW, LL, JL, DC and LS.



Competing interests

410 The authors declare that they have no conflict of interest.

Acknowledgements

This research was supported by the New Zealand Agricultural Greenhouse Gas Research Centre (NZAGRC), AgResearch Ruakura, DairyNZ and the University of Waikato. The authors would like to recognise the farm owners, Sarah and Ben Troughton, for their cooperation. Chris Morcom is thanked for his help in the fields and Emily Huang from NZ-NCNM for
 415 her all-embracing support regarding gas chromatography. Training notes on the concept of bioequivalence were gratefully received from Neil Cox. We would like to further acknowledge the continuous support from Aerodyne Research Ltd. in maintaining and advancing our QCL based EC systems. Finally, Cecile A. M. de Klein, Tom P. Moore and other (anonymous) reviewers are thanked for thoroughly revising the manuscript of this work.

References

- 420 Baldocchi, D.: Measuring fluxes of trace gases and energy between ecosystems and the atmosphere – the state and future of the eddy covariance method, *Global Change Biol.*, 20, 3600-3609, 10.1111/gcb.12649, 2014.
- Bland, M. J., and Altman, D. G.: Statistical method for assessing agreement between two methods of clinical measurement, *The Lancet*, 327, 307-310, [https://doi.org/10.1016/S0140-6736\(86\)90837-8](https://doi.org/10.1016/S0140-6736(86)90837-8), 1986.
- Bouwman, A. F., Boumans, L. J. M., and Batjes, N. H.: Emissions of N₂O and NO from fertilized fields: Summary of available measurement data, *Global Biogeochem. Cycles*, 16, 6-1, 2002.
- 425 Brümmer, C., Lyshede, B., Lempio, D., Delorme, J.-P., Rüffer, J. J., Fuß, R., Moffat, A. M., Hurkuck, M., Ibrom, A., Ambus, P., Flessa, H., and Kutsch, W. L.: Gas chromatography vs. quantum cascade laser-based N₂O flux measurements using a novel chamber design, *Biogeosciences*, 14, 1365-1381, 10.5194/bg-14-1365-2017, 2017.
- Butterbach-Bahl, K., Baggs, E. M., Dannenmann, M., Kiese, R., and Zechmeister-Boltenstern, S.: Nitrous oxide emissions from soils: how well do we understand the processes and their controls?, *Philosophical transactions of the Royal Society of London. Series B, Biological sciences*, 368, 20130122, 10.1098/rstb.2013.0122, 2013.
- 430 Cardenas, L. M., Bhogal, A., Chadwick, D. R., McGeough, K., Misselbrook, T., Rees, R. M., Thorman, R. E., Watson, C. J., Williams, J. R., Smith, K. A., and Calvet, S.: Nitrogen use efficiency and nitrous oxide emissions from five UK fertilised grasslands, *Sci. Total Environ.*, 10.1016/j.scitotenv.2019.01.082, 2019.
- 435 Chadwick, D. R., Cardenas, L., Misselbrook, T. H., Smith, K. A., Rees, R. M., Watson, C. J., McGeough, K. L., Williams, J. R., Cloy, J. M., Thorman, R. E., and Dhanoa, M. S.: Optimizing chamber methods for measuring nitrous oxide emissions from plot-based agricultural experiments, *Eur. J. Soil Sci.*, 65, 295-307, 10.1111/ejss.12117, 2014.
- Christiansen, J. R., Korhonen, J. F. J., Juszczak, R., Giebels, M., and Pihlatie, M.: Assessing the effects of chamber placement, manual sampling and headspace mixing on CH₄ fluxes in a laboratory experiment, *Plant and Soil*, 343, 171-185, 10.1007/s11104-010-0701-y, 2011.



- Christiansen, J. R., Outhwaite, J., and Smukler, S. M.: Comparison of CO₂, CH₄ and N₂O soil-atmosphere exchange measured in static chambers with cavity ring-down spectroscopy and gas chromatography, *Agric. For. Meteorol.*, 211-212, 48-57, <https://doi.org/10.1016/j.agrformet.2015.06.004>, 2015.
- Cowan, N., Levy, P., Maire, J., Coyle, M., Leeson, S. R., Famulari, D., Carozzi, M., Nemitz, E., and Skiba, U.: An evaluation of four years of nitrous oxide fluxes after application of ammonium nitrate and urea fertilisers measured using the eddy covariance method, *Agric. For. Meteorol.*, 280, 107812, <https://doi.org/10.1016/j.agrformet.2019.107812>, 2020.
- Cowan, N. J., Famulari, D., Levy, P. E., Anderson, M., Bell, M. J., Rees, R. M., Reay, D. S., and Skiba, U. M.: An improved method for measuring soil N₂O fluxes using a quantum cascade laser with a dynamic chamber, *Eur. J. Soil Sci.*, 65, 643-652, 10.1111/ejss.12168, 2014.
- Curl, R. F., Capasso, F., Gmachl, C., Kosterev, A. A., McManus, B., Lewicki, R., Pusharsky, M., Wysocki, G., and Tittel, F. K.: Quantum cascade lasers in chemical physics, *Chem. Phys. Lett.*, 487, 1-18, <https://doi.org/10.1016/j.cplett.2009.12.073>, 2010.
- de Klein, C. A. M., Barton, L., Sherlock, R. R., Li, Z., and Littlejohn, R. P.: Estimating a nitrous oxide emission factor for animal urine from some New Zealand pastoral soils, *Aust. J. Soil Res.*, 41, 381-399, 10.1071/SR02128, 2003.
- de Klein, C. A. M., Harvey, M. J., Clough, T., Rochette, P., Kelliher, F., Venetera, R., Alfaro, M., and Chadwick, D.: Nitrous Oxide Chamber Methodology Guidelines. Version 1.1, Ministry of Primary Industries., Wellington, 146, 2015.
- Denmead, O.: Approaches to measuring fluxes of methane and nitrous oxide between landscapes and the atmosphere, *Plant and Soil*, 309, 5-24, 10.1007/s11104-008-9599-z, 2008.
- Erisman, J. W., Galloway, J. N., Seitzinger, S., Bleeker, A., Dise, N. B., Petrescu, A. M. R., Leach, A. M., and de Vries, W.: Consequences of human modification of the global nitrogen cycle, *Philosophical Transactions of the Royal Society B: Biological Sciences*, 368, 10.1098/rstb.2013.0116, 2013.
- Faust, D. R., and Liebig, M. A.: Effects of storage time and temperature on greenhouse gas samples in Exetainer vials with chlorobutyl septa caps, *MethodsX*, 5, 857-864, <https://doi.org/10.1016/j.mex.2018.06.016>, 2018.
- Firestone, M. K., and Davidson, E. A.: Microbiological Basis of NO and N₂O Production and Consumption in Soil, in: *Exchange of Trace Gases between Terrestrial Ecosystems and the Atmosphere*, edited by: Andreae, M. O., and Schimmel, D. S., John Wiley & Sons Ltd, 7-21, 1989.
- Flechard, C. R., Ambus, P., Skiba, U., Rees, R. M., Hensen, A., van Amstel, A., van Den Pol-van Dasselaar, A., Soussana, J. F., Jones, M., Clifton-Brown, J., Raschi, A., Horvath, L., Neftel, A., Jocher, M., Ammann, C., Leifeld, J., Fuhrer, J., Calanca, P., Thalman, E., Pilegaard, K., Di Marco, C., Campbell, C., Nemitz, E., Hargreaves, K. J., Levy, P. E., Ball, B. C., Jones, S. K., van de Bulk, W. C. M., Groot, T., Blom, M., Domingues, R., Kasper, G., Allard, V., Ceschia, E., Cellier, P., Laville, P., Henault, C., Bizouard, F., Abdalla, M., Williams, M., Baronti, S., Berretti, F., and Grosz, B.: Effects of climate and management intensity on nitrous oxide emissions in grassland systems across Europe, *Agriculture, Ecosystems and Environment*, 121, 135-152, 10.1016/j.agee.2006.12.024, 2007.
- Giavarina, D.: Understanding Bland Altman analysis, *Biochemia medica*, 25, 141-151, 10.11613/BM.2015.015, 2015.
- Hutchinson, G. L., and Mosier, A. R.: Improved Soil Cover Method for Field Measurement of Nitrous Oxide Fluxes¹, *Soil Sci. Soc. Am. J.*, 45, 311-316, 10.2136/sssaj1981.03615995004500020017x, 1981.
- IPCC: Anthropogenic and Natural Radiative Forcing, in: *Climate Change 2013: The Physical Science Basis. Contribution of Working Group I to the Fifth Assessment Report of the Intergovernmental Panel on Climate Change.*, edited by: Myhre, G., Shindell, D., Breon, F.-M., Collins, W., Fuglestedt, J., Huang, J., Koch, D., Lamarque, J.-F., Lee, D., Mendoza, B., Nakajima, T., Robock, A., Stephens, G., Takemura, T., Zhang, H., Jacob, D., Ravishankara, A. R., and Shine, K. P., Cambridge UK and New York, NY, USA, 659-740, 2013.



- Jones, S., Famulari, D., Marco, C., Nemitz, E., Skiba, U., Rees, R., and Sutton, M.: Nitrous oxide emissions from managed grassland: a comparison of eddy covariance and static chamber measurements, *Atmos. Meas. Tech.*, 4, 2179–2194, 10.5194/amt-4-2179-2011, 2011.
- 480 Jones, S. K., Rees, R. M., Skiba, U. M., and Ball, B. C.: Influence of organic and mineral N fertiliser on N₂O fluxes from a temperate grassland, *Agriculture, Ecosystems and Environment*, 121, 74–83, 10.1016/j.agee.2006.12.006, 2007.
- Kroon, P., Hensen, A., Bulk, W., Jongejan, P., and Vermeulen, A.: The importance of reducing the systematic error due to non-linearity in N₂O flux measurements by static chambers, *Nutr. Cycling Agroecosyst.*, 82, 175–186, 10.1007/s10705-008-9179-x, 2008.
- 485 Lammirato, C., Lebender, U., Tierling, J., and Lammel, J.: Analysis of uncertainty for N₂O fluxes measured with the closed-chamber method under field conditions: Calculation method, detection limit, and spatial variability, *J. Plant Nutr. Soil Sci.*, 181, 78–89, 10.1002/jpln.201600499, 2018.
- Lebague, B., Schmidt, M., Ramonet, M., Wastine, B., Yver Kwok, C., Laurent, O., Belviso, S., Guemri, A., Philippon, C., Smith, J., and Conil, S.: Comparison of N₂O analyzers for high-precision measurements of atmospheric mole fractions, *Atmos. Meas. Tech.*, 9, 1221–1238, 10.5194/amt-9-1221-2016, 2016.
- 490 Liáng, L. L., Campbell, D. I., Wall, A. M., and Schipper, L. A.: Nitrous oxide fluxes determined by continuous eddy covariance measurements from intensively grazed pastures: Temporal patterns and environmental controls, *Agriculture, Ecosystems & Environment*, 268, 171–180, <https://doi.org/10.1016/j.agee.2018.09.010>, 2018.
- Lundegard, H.: Carbon dioxide evolution of soil and crop growth, *Soil Science*, 23, 417–453, 1927.
- Luo, J., Ledgard, S. F., and Lindsey, S. B.: Nitrous oxide emissions from application of urea on New Zealand pasture, *N.Z. J. Agric. Res.*, 50, 1–11, 10.1080/00288230709510277, 2007.
- 495 Luo, J., Ledgard, S., Klein, C., Lindsey, S., and Kear, M.: Effects of dairy farming intensification on nitrous oxide emissions, *Plant Soil*, 309, 227–237, 10.1007/s11104-007-9444-9, 2008a.
- Luo, J., Lindsey, S., and Ledgard, S.: Nitrous oxide emissions from animal urine application on a New Zealand pasture, *Biol. Fertil. Soils*, 44, 463–470, 10.1007/s00374-007-0228-4, 2008b.
- 500 Luo, J., Wyatt, J., van der Weerden, T. J., Thomas, S. M., de Klein, C. A. M., Li, Y., Rollo, M., Lindsey, S., Ledgard, S. F., Li, J., Ding, W., Qin, S., Zhang, N., Bolan, N. S., Kirkham, M. B., Bai, Z., Ma, L., Zhang, X., Wang, H., Liu, H., and Rys, G.: Potential Hotspot Areas of Nitrous Oxide Emissions From Grazed Pastoral Dairy Farm Systems, *Advances in Agronomy*, 145, 205–268, 10.1016/bs.agron.2017.05.006, 2017.
- Mulvaney, R. L.: Extraction of exchangeable ammonium, nitrate and nitrite, in: *Methods of soil analysis Part 3: chemical methods*, edited by: Sparks, D. L., Page, A. L., Helmke, P. A., and Loeppert, R. H., 5.3, Soil Science Society of America, American Society of Agronomy, Madison, WI, 1129–1131, 1996.
- 505 Neftel, A., Flechard, C., Ammann, C., Conen, F., Emmenegger, L., and Zeyer, K.: Experimental assessment of N₂O background fluxes in grassland systems, *Tellus B Chem Phys Meteorol*, 59, 470–482, 10.1111/j.1600-0889.2007.00273.x, 2007.
- Nelson, D. D., McManus, B., Urbanski, S., Herndon, S., and Zahniser, M. S.: High precision measurements of atmospheric nitrous oxide and methane using thermoelectrically cooled mid-infrared quantum cascade lasers and detectors, *Spectrochim. Acta, Part A*, 60, 3325–3335, <https://doi.org/10.1016/j.saa.2004.01.033>, 2004.
- 510 Nemitz, E., Mammarella, I., Ibrom, A., Aurela, M., Burba, G., Dengel, S., Gielen, B., Grelle, A., Heinesch, B., Herbst, M., Hörtnagl, L., Klemetsson, L., Lindroth, A., Lohila, A., McDermitt, K. D., Meier, P., Merbold, L., Nelson, D., Nicolini, G., and Zahniser, M.: Standardisation of eddy-covariance flux measurements of methane and nitrous oxide, 32, 517–549, 10.1515/intag-2017-0042, 2018.



- 515 Nicolini, G., Castaldi, S., Fratini, G., and Valentini, R.: A literature overview of micrometeorological CH₄ and N₂O flux measurements in terrestrial ecosystems, *Atmos. Environ.*, 81, 311-319, <https://doi.org/10.1016/j.atmosenv.2013.09.030>, 2013.
- National Climate Database. National Institute of Water and Atmospheric Research: <http://cliflo.niwa.co.nz/>, 2018.
- Parkin, T. B., and Venterea, R. T.: Chamber-based trace gas flux measurements, USDA-ARS GRACEnet Project Protocols, Chapter 3, 2010.
- Parkin, T. B., Venterea, R. T., and Hargreaves, S. K.: Calculating the Detection Limits of Chamber-based Soil Greenhouse Gas Flux Measurements, *J. Environ. Qual.*, 41, 705-715, [10.2134/jeq2011.0394](https://doi.org/10.2134/jeq2011.0394), 2012.
- 520 Patterson, S., and Jones, B.: Interdisciplinary statistics. Bioequivalence and statistics in clinical pharmacology, Taylor & Francis Group, Boca Raton, FL, 2006.
- Pavelka, M., Acosta, M., Kiese, R., Altimir, N., Bruemmer, C., Crill, P., Darenova, E., Fuß, R., Gielen, B., Graf, A., Klemetsson, L., Lohila, A., Longdoz, B., Lindroth, A., Nilsson, M., Marañón-Jiménez, S., Merbold, L., Montagnani, L., Peichl, M., and Kutsch, W. L.: Standardisation of chamber technique for CO₂, N₂O and CH₄ fluxes measurements from terrestrial ecosystems, *Int. Agrophys.*, 32, 569-587, [10.1515/intag-2017-0045](https://doi.org/10.1515/intag-2017-0045), 2018.
- 525 Rani, S., and Pargal, A.: Bioequivalence: An overview of statistical concepts, *Indian Journal of Pharmacology*, 36, 209-216, 2004.
- Rannik, Ü., Haapanala, S., Shurpali, N. J., Mammarella, I., Lind, S., Hyvönen, N., Peltola, O., Zahniser, M., Martikainen, P. J., and Vesala, T.: Intercomparison of fast response commercial gas analysers for nitrous oxide flux measurements under field conditions, *Biogeosciences*, 12, 415-432, [10.5194/bg-12-415-2015](https://doi.org/10.5194/bg-12-415-2015), 2015.
- 530 Rapson, T. D., and Dacres, H.: Analytical techniques for measuring nitrous oxide, "TrAC, Trends Anal. Chem.", 54, 65-74, [http://dx.doi.org/10.1016/j.trac.2013.11.004](https://doi.org/10.1016/j.trac.2013.11.004), 2014.
- Ravishankara, J. S., Daniel, R. W., and Portmann, R. W.: Nitrous oxide (N₂O): The dominant ozone-depleting substance emitted in the 21st century, *Science*, 326, 123-125, [10.1126/science.1176985](https://doi.org/10.1126/science.1176985), 2009.
- Reay, D. S., Davidson, E. A., Smith, K. A., Smith, P., Melillo, J. M., Dentener, F., and Crutzen, P. J.: Global agriculture and nitrous oxide emissions, *Nature Climate Change*, 2, 410, [10.1038/nclimate1458](https://doi.org/10.1038/nclimate1458)
- 535 <https://www.nature.com/articles/nclimate1458#supplementary-information>, 2012.
- Rees, R., Augustin, J., Alberti, G., Ball, B., Boeckx, P., Cantarel, A., Castaldi, S., Chirinda, N., Chojnicki, B., Giebels, M., Gordon, H., Grosz, B., Horvath, L., Juszczak, R., Klemetsson, Å., Klemetsson, L., Medinets, S., Machon, A., Mapanda, F., Nyamangara, J., Olesen, J., Reay, D., Sanchez, L., Cobena, A., Smith, K., Sowerby, A., Sommer, M., Soussana, J., Stenberg, M., Topp, C., van Cleemput, O., Vallejo, A., Watson, C., and Wuta, M.: Nitrous oxide emissions from European agriculture - an analysis of variability and drivers of emissions from
- 540 field experiments, *Biogeosciences*, 10, 2671, [10.5194/bg-10-2671-2013](https://doi.org/10.5194/bg-10-2671-2013), 2013.
- Ring, A., Lang, B., Kazaroho, C., Labes, D., Schall, R., and Schütz, H.: Sample size determination in bioequivalence studies using statistical assurance, *British Journal of Clinical Pharmacology*, 85, 2369-2377, [10.1111/bcp.14055](https://doi.org/10.1111/bcp.14055), 2019.
- Rochette, P., and Bertrand, N.: Soil air sample storage and handling using polypropylene syringes and glass vials, *Can. J. Soil Sci.*, 83, 631-637, [10.4141/S03-015](https://doi.org/10.4141/S03-015), 2003.
- 545 Rochette, P., and Eriksen-Hamel, N.: Chamber Measurements of Soil Nitrous Oxide Flux: Are Absolute Values Reliable?, *Soil Sci. Soc. Am. J.*, 72, 331-342, [10.2136/sssaj2007.0215](https://doi.org/10.2136/sssaj2007.0215), 2008.
- Rochette, P.: Towards a standard non-steady-state chamber methodology for measuring soil N₂O emissions, *Anim. Feed Sci. Technol.*, 166, 141-146, [http://dx.doi.org/10.1016/j.anifeedsci.2011.04.063](https://doi.org/10.1016/j.anifeedsci.2011.04.063), 2011.



- 550 Rosenstock, T. S., Diaz-Pines, E., Zuazo, P., Jordan, G., Predotova, M., Mutuo, P., Abwanda, S., Thiong'o, M., Buerkert, A., Rufino, M. C., Kiese, R., Neufeldt, H., and Butterbach-Bahl, K.: Accuracy and precision of photoacoustic spectroscopy not guaranteed, *Global Change Biol.*, 19, 3565-3567, 10.1111/gcb.12332, 2013.
- Savage, K., Phillips, R., and Davidson, E.: High temporal frequency measurements of greenhouse gas emissions from soils, *Biogeosciences*, 11, 2709-2720, 10.5194/bg-11-2709-2014, 2014.
- 555 Tallec, T., Brut, A., Joly, L., Dumelié, N., Serça, D., Mordelet, P., Claverie, N., Legain, D., Barrié, J., Decarpenterie, T., Cousin, J., Zawilski, B., Ceschia, E., Guérin, F., and Le Dantec, V.: N₂O flux measurements over an irrigated maize crop: A comparison of three methods, *Agric. For. Meteorol.*, 264, 56-72, <https://doi.org/10.1016/j.agrformet.2018.09.017>, 2019.
- Thompson, R. L., Lassaletta, L., Patra, P. K., Wilson, C., Wells, K. C., Gressent, A., Koffi, E. N., Chipperfield, M. P., Winiwarter, W., Davidson, E. A., Tian, H., and Canadell, J. G.: Acceleration of global N₂O emissions seen from two decades of atmospheric inversion, *Nature Climate Change*, 10.1038/s41558-019-0613-7, 2019.
- 560 van der Laan, S., Neubert, R. E. M., and Meijer, H. A. J.: A single gas chromatograph for accurate atmospheric mixing ratio measurements of CO₂, CH₄, N₂O, SF₆ and CO, *Atmos. Meas. Tech.*, 2, 549-559, 2009.
- van der Weerden, T. J., Luo, J., de Klein, C. A. M., Hoogendoorn, C. J., Littlejohn, R. P., and Rys, G. J.: Disaggregating nitrous oxide emission factors for ruminant urine and dung deposited onto pastoral soils, *Agriculture, Ecosystems and Environment*, 141, 426-436, 10.1016/j.agee.2011.04.007, 2011.
- 565 van der Weerden, T. J., Clough, T. J., and Styles, T. M.: Using near-continuous measurements of N₂O emission from urine-affected soil to guide manual gas sampling regimes, *N.Z. J. Agric. Res.*, 56, 60-76, 10.1080/00288233.2012.747548, 2013.
- Velthof, G. L., Jarvis, S. C., Stein, A., Allen, A. G., and Oenema, O.: Spatial variability of nitrous oxide fluxes in mown and grazed grasslands on a poorly drained clay soil, *Soil Biol. Biochem.*, 28, 1215-1225, [https://doi.org/10.1016/0038-0717\(96\)00129-0](https://doi.org/10.1016/0038-0717(96)00129-0), 1996.
- 570 Wecking, A. R., Wall, A. M., Liáng, L. L., Lindsey, S. B., Luo, J., Campbell, D. I., and Schipper, L. A.: Reconciling annual nitrous oxide emissions of an intensively grazed dairy pasture determined by eddy covariance and emission factors, *Agriculture, Ecosystems & Environment*, 287, 106646, <https://doi.org/10.1016/j.agee.2019.106646>, 2020a.
- Wecking, A. R., Wall, A. M., Liáng, L. L., Lindsey, S. B., Luo, J., Campbell, D. I., and Schipper, L. A.: Dataset for “A novel injection technique: using a field-based quantum cascade laser for the analysis of gas samples derived from static chamber”. <https://researchcommons.waikato.ac.nz/handle/10289/13539>, 2020b.
- 575 Westlake, W. J.: Bioavailability and bioequivalence of pharmaceutical formulations, in: *Biopharmaceutical Statistics for Drug Development*, edited by: Peace, K. E., Marcel Dekker, New York, 329-352, 1988.
- Zellweger, C., Steinbrecher, R., Laurent, O., Lee, H., Kim, S., Emmenegger, L., Steinbacher, M., and Buchmann, B.: Recent advances in measurement techniques for atmospheric carbon monoxide and nitrous oxide observations, *Atmos. Meas. Tech.*, 12, 5863-5878, 10.5194/amt-12-5863-2019, 2019.
- 580



List of figures

Figure 1: Schematic illustration of how to use a field-based QCL for EC measurements and manual injections. (1) shows the main components of the QCL EC system; (2) provides an example of a static chamber from which N₂O samples were taken and stored in (3) pre-evacuated glass vials. Once the set-up for manual injections (4) was assembled and the QCL air-inlet (5) adjusted from drawing ambient air through the EC sample line (inlet 1) to drawing air through the injection tube (inlet 2), the QCL was readily set-up for receiving injections of N₂O samples and associated standards through the injection port. The data output (6) was immediate allowing processing and data evaluation on the day of chamber sampling.

Figure 2: Fluxes of nitrous oxide (F_{N₂O}) determined from (a) gas chromatography (F_{N₂O_GC}) and (b) quantum cascade laser absorption spectrometry (F_{N₂O_QCL}). Symbols depict mean F_{N₂O} and marker shading displays the rate of ammonium nitrate (AN) applied: AN₀ (black squares), AN₃₀₀ (dark grey diamonds), AN₆₀₀ (light grey upside-down triangles) and AN₉₀₀ (white triangles). Error bars illustrate the standard error of the mean (SEM) across the three replicates of the same treatment. Note that flux measurements on 12 and 15 September were conducted twice daily (10 AM and 12 PM) and that the time scale on the x-axis, therefore, is discrete. Soil water-filled pore space and mineral nitrogen contents associated with flux measurements are provided in the supplementary material, Table S3.

Figure 3: Orthogonal regression analysis of standardised N₂O concentrations (C_{N₂O}) and fluxes (F_{N₂O}). Data were distinguished by their analytic source of origin, i.e. GC (C_{N₂O_GC}, F_{N₂O_GC}) and QCL (C_{N₂O_QCL}, F_{N₂O_QCL}). The regression analysis included all C_{N₂O} in (a) but only those C_{N₂O} measured at control sites (AN₀) in panel (c). The orthogonal regression analysis was repeated for standardised F_{N₂O} with (b) showing all F_{N₂O_GC} and F_{N₂O_QCL}, and (d) depicting the orthogonal regression for AN₀ fluxes only. Ordinary least squares (dotted light grey line) resulted from the regression of Y on X; inverse least squares from the regression of X on Y (long dotted dark grey line). The major axis (black line) based on orthogonal regression of Y and X using a principal component analysis. Here, the squared residuals perpendicular to the line are minimised. Note, for the purpose of illustration axes in panel (c) and (d) have different scales. Table S4 in the supplements provides further results.

Figure 4: Bland Altman plots of the differences between the GC and QCL method expressed as the percentage difference of the standard method A (F_{N₂O_GC}) and the new method B (F_{N₂O_QCL}) on the y-axis [$((A-B)/\text{mean}) \times 100$] versus the mean of A and B on the x-axis. The limits of agreement are represented by continuous lines at ± 1.96 standard deviation (SD) of the percentage difference. The inset (panel b) illustrates the same data but excludes F_{N₂O_GC} and F_{N₂O_QCL} from control (AN₀) sites. The percentage mean difference (bias) between F_{N₂O_GC} and F_{N₂O_QCL}, i.e. method A and B, is indicated by the gap between the dashed line (line of equality, which is not at zero) and an imaginary line parallel to the dashed line at y = 0. This figure is



based on individual F_{N_2O} (all treatment replicates). Results for mean F_{N_2O} across replicates of the same treatment are provided
 615 in the supplements, see Table S5.

Figure 5: Cumulative emissions of N_2O from each treatment (AN_{300} , AN_{600} , AN_{900}) and the control (AN_0) in $kg\ N_2O-N\ ha^{-1}$
 at the end of the campaign. Data are distinguished into GC (black bars) and QCL (grey bars) budgets. Error bars quantify the
 standard error of the mean (SEM). The absolute difference in $kg\ N_2O-N\ ha^{-1}$ between the two budgets (GC-QCL) is highlighted
 620 by the number at the top of each bar-couple.

Figure 6: Bioequivalence analysis for N_2O concentrations (C_{N_2O}) in (a-d) and N_2O fluxes (F_{N_2O}) in (e) with GC defined as the
 standard method. C_{N_2O} and F_{N_2O} based on QCL analysis were considered bioequivalent when the 90% confidence interval (CI)
 of the difference between QCL and GC (x-axis) was completely within the predefined $\pm 5\%$ bioequivalence range of the
 difference of the standard method. The bioequivalence analysis was distinguished for C_{N_2O} by sampling interval (t_0 , t_{15} , t_{30} ,
 625 t_{45}) and treatment with panel (a) showing results for control sites (AN_0) and panels (b), (c) and (d) for AN_{300} , AN_{600} and AN_{900}
 treatment sites. Similarly, a bioequivalence analysis was determined for F_{N_2O} in panel (e), here distinguished by AN application
 rate on the y-axis.

630 List of tables

Table 1: Comparison of the GC and QCL injection methods. Details provided in the below table specifically relate to the
 application of the two techniques in this study (i.e. have not been generalised). NZD = New Zealand dollars.

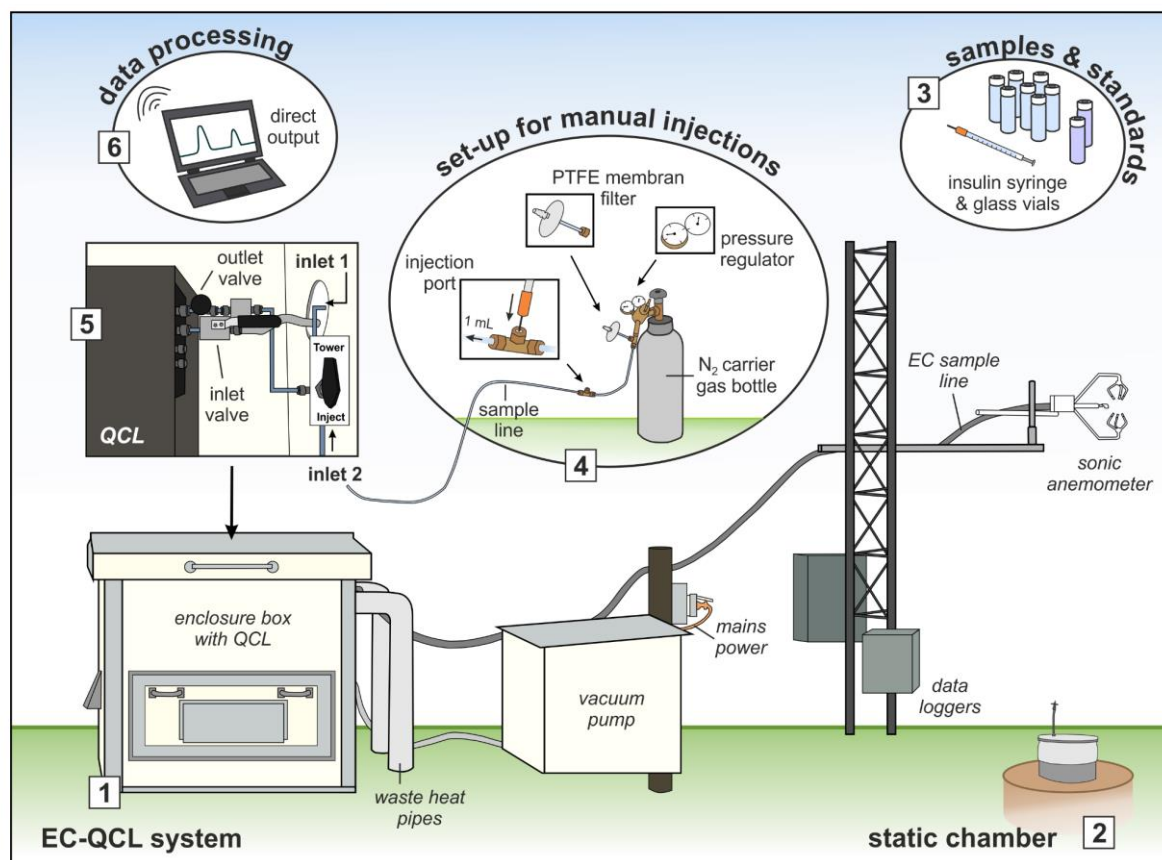


Figure 1: Schematic illustration of how to use a field-based QCL for EC measurements and manual injections. (1) shows the main components of the QCL EC system; (2) provides an example of a static chamber from which N₂O samples were taken and stored in (3) pre-evacuated glass vials. Once the set-up for manual injections (4) was assembled and the QCL air-inlet (5) adjusted from drawing ambient air through the EC sample line (inlet 1) to drawing air through the injection tube (inlet 2), the QCL was readily set-up for receiving injections of N₂O samples and associated standards through the injection port. The data output (6) was immediate allowing processing and data evaluation on the day of chamber sampling.

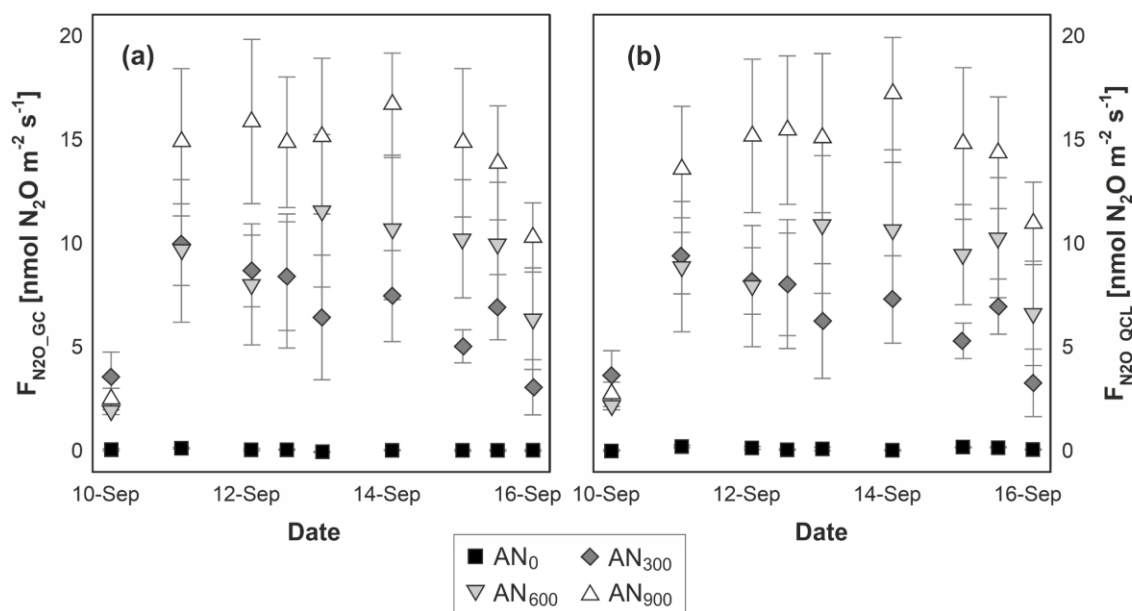


Figure 2: Fluxes of nitrous oxide (F_{N_2O}) determined from (a) gas chromatography ($F_{N_2O_GC}$) and (b) quantum cascade laser absorption spectrometry ($F_{N_2O_QCL}$). Symbols depict mean F_{N_2O} and marker shading displays the rate of ammonium nitrate (AN) applied: AN_0 (black squares), AN_{300} (dark grey diamonds), AN_{600} (light grey upside-down triangles) and AN_{900} (white triangles). Error bars illustrate the standard error of the mean (SEM) across the three replicates of the same treatment. Note that flux measurements on 12 and 15 September were conducted twice daily (10 AM and 12 PM) and that the time scale on the x-axis, therefore, is discrete. Soil water-filled pore space and mineral nitrogen contents associated with flux measurements are provided in the supplementary material, Table S3.

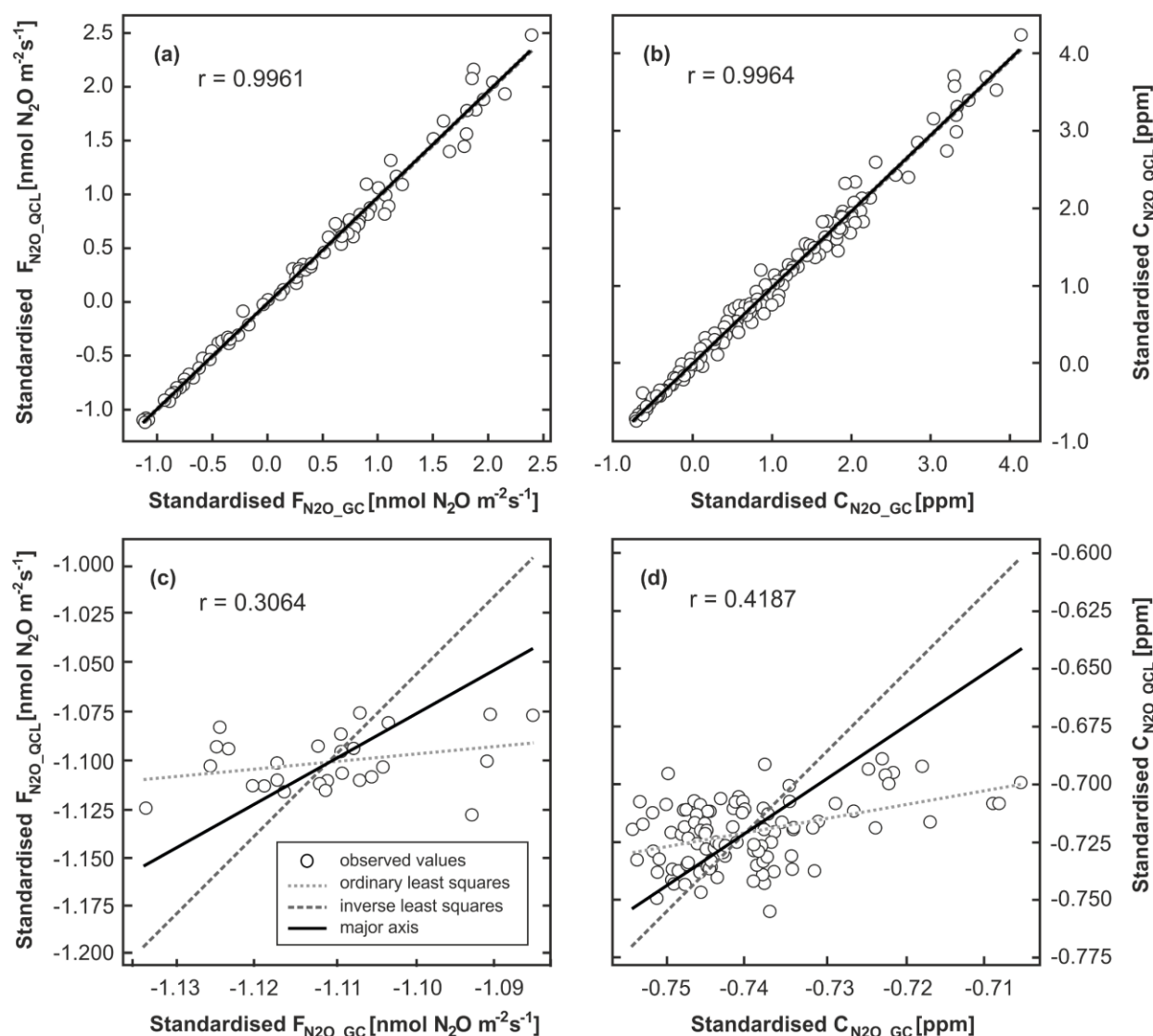
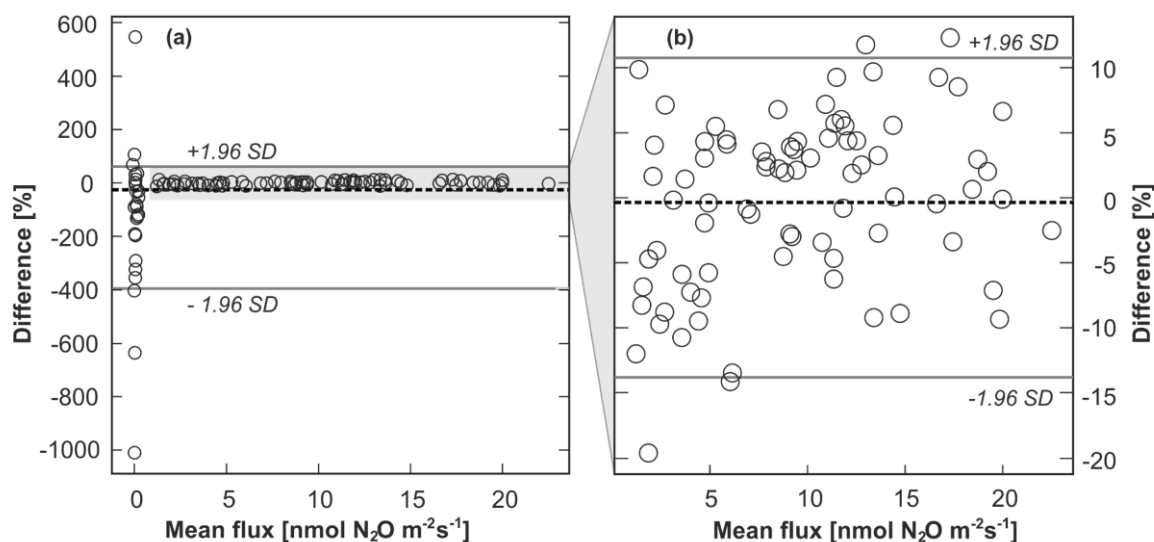
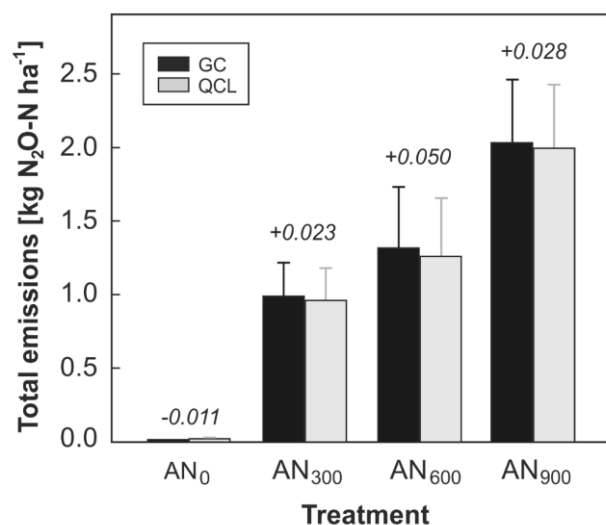


Figure 3: Orthogonal regression analysis of standardised N_2O concentrations ($C_{\text{N}_2\text{O}}$) and fluxes ($F_{\text{N}_2\text{O}}$). Data were distinguished by their analytic source of origin, i.e. GC ($C_{\text{N}_2\text{O_GC}}$, $F_{\text{N}_2\text{O_GC}}$) and QCL ($C_{\text{N}_2\text{O_QCL}}$, $F_{\text{N}_2\text{O_QCL}}$). The regression analysis included all $C_{\text{N}_2\text{O}}$ in (a) but only those $C_{\text{N}_2\text{O}}$ measured at control sites (AN_0) in panel (c). The orthogonal regression analysis was repeated for standardised $F_{\text{N}_2\text{O}}$ with (b) showing all $F_{\text{N}_2\text{O_GC}}$ and $F_{\text{N}_2\text{O_QCL}}$, and (d) depicting the orthogonal regression for AN_0 fluxes only. Ordinary least squares (dotted light grey line) resulted from the regression of Y on X; inverse least squares from the regression of X on Y (long dotted dark grey line). The major axis (black line) based on orthogonal regression of Y and X using a principal component analysis. Here, the squared residuals perpendicular to the line are minimised. Note, for the purpose of illustration axes in panel (c) and (d) have different scales. Table S4 in the supplements provides further results.



665 **Figure 4:** Bland Altman plots of the differences between the GC and QCL method expressed as the percentage difference of
 the standard method A ($F_{N_2O_GC}$) and the new method B ($F_{N_2O_QCL}$) on the y-axis [$((A-B)/\text{mean}) \times 100$] versus the mean of A
 and B on the x-axis. The limits of agreement are represented by continuous lines at ± 1.96 standard deviation (SD) of the
 percentage difference. The inset (panel b) illustrates the same data but excludes $F_{N_2O_GC}$ and $F_{N_2O_QCL}$ from control (AN_0) sites.
 The percentage mean difference (bias) between $F_{N_2O_GC}$ and $F_{N_2O_QCL}$, i.e. method A and B, is indicated by the gap between
 670 the dashed line (line of equality, which is not at zero) and an imaginary line parallel to the dashed line at $y = 0$. This figure is
 based on individual F_{N_2O} (all treatment replicates). Results for mean F_{N_2O} across replicates of the same treatment are provided
 in the supplements, see Table S5.



675

Figure 5: Cumulative emissions of N₂O from each treatment (AN₃₀₀, AN₆₀₀, AN₉₀₀) and the control (AN₀) in kg N₂O-N ha⁻¹ at the end of the campaign. Data are distinguished into GC (black bars) and QCL (grey bars) budgets. Error bars quantify the standard error of the mean (SEM). The absolute difference in kg N₂O-N ha⁻¹ between the two budgets (GC-QCL) is highlighted by the number at the top of each bar-couple.

680

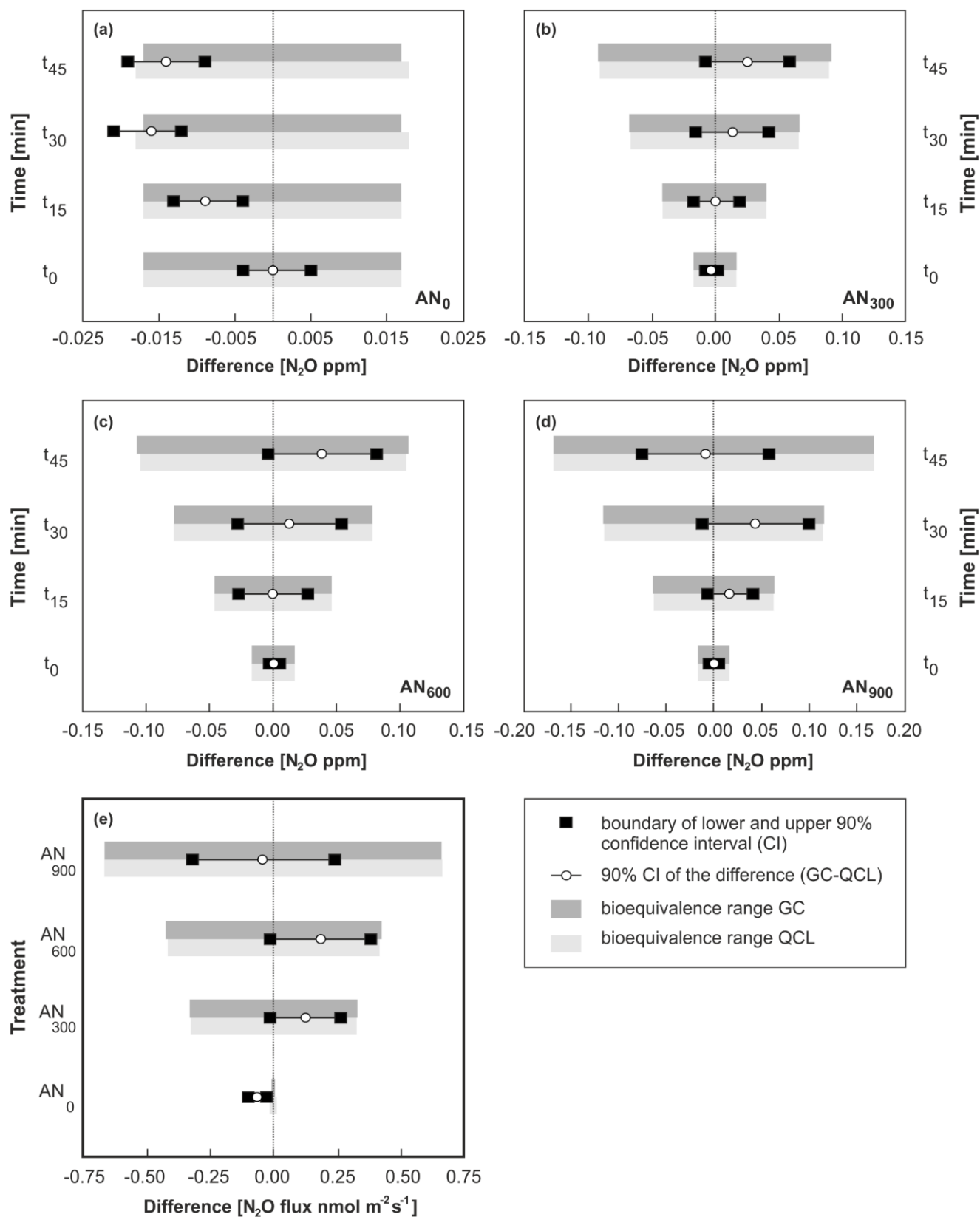




Figure 6: Bioequivalence analysis for N_2O concentrations (C_{N_2O}) in (a-d) and N_2O fluxes (F_{N_2O}) in (e) with GC defined as the standard method. C_{N_2O} and F_{N_2O} based on QCL analysis were considered bioequivalent when the 90% confidence interval (CI) of the difference between QCL and GC (x-axis) was completely within the predefined $\pm 5\%$ bioequivalence range of the difference of the standard method. The bioequivalence analysis was distinguished for C_{N_2O} by sampling interval (t_0 , t_{15} , t_{30} , t_{45}) and treatment with panel (a) showing results for control sites (AN_0) and panels (b), (c) and (d) for AN_{300} , AN_{600} and AN_{900} treatment sites. Similarly, a bioequivalence analysis was determined for F_{N_2O} in panel (e), here distinguished by AN application rate on the y-axis.

690

Table 1: Comparison of the GC and QCL injection methods. Details provided in the below table specifically relate to the application of the two techniques in this study (i.e. have not been generalised). NZD = New Zealand dollars.

	GC	QCL
Capital cost per device (NZD)	40,000	160,000
Labour effort for preparation and data processing of 100 samples (hours)	2 to 3	< 1
Transport of samples	required	not required
Storage of samples	required	optional
Analysis location	lab-based	field-based
Analysis time (days)	multiple days	immediate
Analysis cost per sample (NZD)	3.5	< 0.5
Possible injections (per hour)	7.5	~200
Lag time between injections (sec)	480	< 10
Injection procedure	manual/automated	manual
Injection of N_2O standards	required	required
Injection volume per sample (mL)	6	1
Carrier gas	N_2	N_2
Flow rate ($L\ min^{-1}$)	0.4	1
Output of result data	post analysis	immediate